# Selective Reduction of Formamides to *O*-silylated hemiaminals or methylamines with $HSiMe_2Ph$ Catalyzed by Iridium Complexes

Jefferson Guzmán, Ana M. Bernal, Pilar García-Orduña, Fernando J. Lahoz, Luis A. Oro and Francisco J. Fernández-Alvarez*

The reaction of (4-methyl-pyridin-2-iloxy)ditertbutylsilane ($NSi^{tBu}$-H, **1**) with $[IrCl(coe)_2]_2$ affords the iridium(III) complex $[Ir(H)(Cl)(\kappa^2\text{-}NSi^{tBu})(coe)]$ (**2**), which has been fully characterized including X-ray diffraction studies. The reaction of **2** with $AgCF_3SO_3$ leads to the formation of species $[Ir(H)(CF_3SO_3)(\kappa^2\text{-}NSi^{tBu})(coe)]$ (**3**). The iridium complexes **2** and **3** are effective catalyst for the reduction of formamides with $HSiMe_2Ph$. The selectivity of the redution procees depends on the catalyst. Thus, using complex **2**, with a chloride ancyllary ligand, it has been possible to selectively obtain the corresponding corresponding *O*-silylated hemiaminal by reaction of formamides with one equivalent of $HSiMe_2Ph$, while complex **3**, with a triflate ligand instead of chloride, catalyzed the selective reduction of formamides to the corresponding methylamine.

## Introduction

Amines are chemicals of great interest due to their numerous and different applications.[1] They have been commonly prepared by stoichiometric reduction of amides with metal hydrides. However, the application of this type of reducing agents at industrial scale faces two main issues: i) the generation of huge amounts of residues, and ii) the fact that metal hydrides are moisture and air sensitive.[2] That is why the development of catalytic systems allowing the selective reduction of amides under mild reaction conditions constitutes an interesting research field. During the last years, some examples of efficient homogeneous catalysts for the reduction of amides to amines using hydrogen, hydroboranes or hydrosilanes as reducing agents have been reported.[3] In this context, the catalytic hydrosilylation of amides has emerged as a chemical technology for the synthesis of amines with siloxanes as the only side reaction products.[3i,3j]

To the best of our knowledge, the first examples of catalytic reduction of amides to amines, using hydrosilanes as reductants, were reported in 1962 by Calas et al.[4] They used $ZnCl_2$ as catalyst for the reduction of $RCONEt_2$ (R = Me, Et, Pr, Ph) to the corresponding amine using $HSiEt_3$ as reducing agent, the reaction required to heat at 418K for 3 days to achieved a 60-87% yield.[4] In 1998, Ito and collaborators reported that the complex $[RhCl(CO)(PPh_3)_3]$ (0.1 mol%) catalyzed the reduction of tertiary amides with 2.1-2.5 equiv. of $H_2SiEt_2$ to yield the corresponding tertiary amine.[5] Since then, several examples of catalysts based on Ti,[6] Mo,[7] Fe,[8] Ru,[9] Co,[10] Rh,[5,11] Ir,[12] Pt,[13] Cu,[14] or Zn[15] complexes effective for the reduction of amides to the corresponding amine using silicon-hydrides as reductants have been published.

In this context, as a continuation of our studies on the application of iridium systems as homogeneous catalysts for the reduction of unsaturated organic molecules with hydrosilanes,[16] we have found that iridium(III) species with the monoanionic bidentate (4-methyl-pyridin-2-iloxy)ditertbutylsilyl ($NSi^{tBu}$) ligand are effective catalysts for the reduction of formamides to the corresponding methylamine under mild reaction conditions and low catalyst loading (0.5 mol%). Moreover, the nature of the ancillary ligand influences the selectivity of these Ir-$NSi^{tBu}$ based catalysts, thus using the chloride derivative it has been possible to selectively reduce formamides to the corresponding *O*-silylated hemiaminal, while Ir-$NSi^{tBu}$ catalysts bearing a triflate ligand catalyzed the selective reduction of formamides to the corresponding methylamine.

## Results and discussion

### Synthesis and characterization of the catalyst precursors

During recent years we have explored the potential of iridium[17-20] and rhodium[21] complexes with monoanionic tridentate NSiN ligands as hydrosilylation or silylation catalysts. The presence of the silyl group labilizes the interaction of the metal with the substrate *trans* located to the silicon atom, which positively influences the catalytic activity of these species (Scheme 1).[16] However, the preference of NSiN ligands for the *fac*-coordination hinder the interaction of the catalytic active site with bulky substrates.

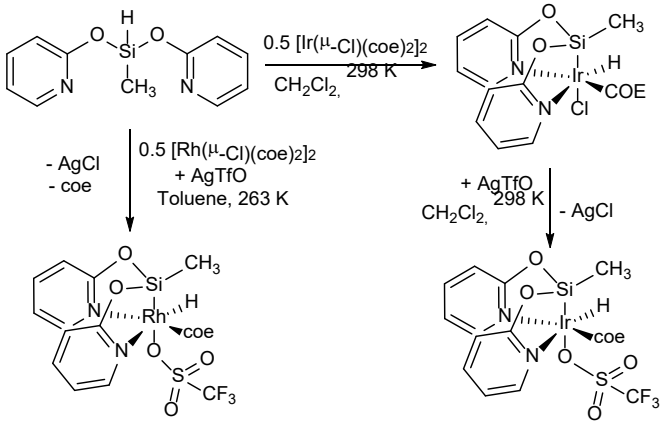


Scheme 1. Examples of synthesis of previously reported Ir-NSiN and Rh-NSiN catalysts precursors.[16]

In this context, it should be mentioned that the chemistry of iridium complexes with pyridine-2-iloxy-silyl based anions as monoanionic bidentate ligands, which could afford less sterically encumbered iridium catalysts, remains unexplored.[22]

In this work, the functionalized hydrosilane 4-methylpyridin-2-iloxy-di*tert*butyl silane (**1**) has been used as ligand precursor. Compound **1** has been obtained in 92% by stirring for 5 hours a mixture of 4-methyl-2-hydroxy-pyridine, $ClSiH^tBu_2$ and imidazole in THF at RT. The reaction of $[IrCl(coe)_2]_2$ (coe = *cis*-

cyclooctene) with two equivalents of freshly prepared **1** in $CH_2Cl_2$ affords the Ir(III) complex [Ir(H)(Cl)($\kappa^2$-NSi$^{tBu}$)(coe)] (**2**) (NSi = 4-methylpyridin-2-iloxy-ditertbutylsilyl), which has been isolated as a yellow solid in 73.4% yield (Scheme 2).

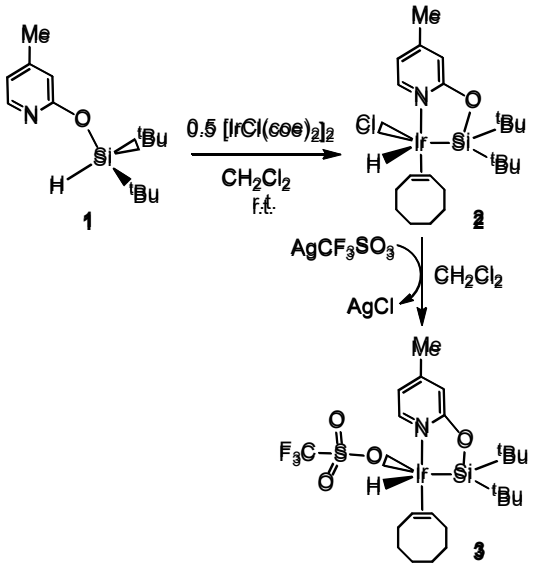


Scheme 2. Synthesis of complexes [Ir(H)(X)($\kappa^2$-NSi$^{tBu}$)(coe)] (X = Cl, **2**; $CF_3SO_3$, **3**).

The iridium complex **2** has been fully characterized by elemental analysis, $^1$H, $^{13}$C{$^1$H} and $^{29}$Si{$^1$H} NMR spectroscopy. In addition, the solid-state structure of **2** has been determined by X-ray diffraction. Complex **2** exhibits a trigonal bipyramidal iridium atom with the nitrogen atom and the centroid of the olefinic bond of cyclooctene at apical positions and equatorial sites occupied by silicon, chloro and hydrogen atoms (Figure 1).

The bidentate coordination of NSi$^{tBu}$ ligand exhibits some similarities with geometrical parameters reported for tridentate NSiN fragments. The nitrogen atom of the NSi$^{tBu}$ fragment is found to be *trans* located to the cyclooctene ligand with Ir-N and Ir-O bond lengths in good agreement with those of [Ir(H)(X)($\kappa^3$-NSiN)(coe)] compounds.[17,20] In fact, the main difference between Ir($\kappa^2$-NSi) bidentate and Ir($\kappa^3$-NSiN) tridentate fragment concerns the Ir-Si bond length, which is found to be longer in complex **2** (2.2853(6) compared to values between 2.2196(14) and 2.2356(12) Å) found for Ir($\kappa^3$-NSiN).[17,20] This feature may be related to a lesser constraint exerted by only one Ir-Si-O-C-N iridacycle in **2**. However, not only the C-O-Si bond angles (close to 120°), but also the iridacycle characteristics are comparable in bidentate and tridentate ligands, as the twisted $^2T_1$ five-membered Ir-Si-O-C-N iridacycle in **2** shows puckering amplitude and phase angle values[23] ($q$= 0.188(1) Å, ϕ= -158.4(1)°) similar to those previously described for [Ir(H)($CF_3CO_2$)($\kappa^3$-NSiN)(coe)][17b] and [Ir(H)($CF_3(CF_2)_2CO_2$)($\kappa^3$-NSiN)(coe)][17a] complexes. Moreover, it should be kept in mind that Ir-Si bond length values in tridentate NSiN complexes are the shortest iridium-silicon bond so far reported in the literature.[24] Electronic effects due to the different metal environment in **2** should not be neglected, although they are not expected to also influence Si-O and Si-C bond lengths, which are found to be longer in **2**. On the contrary, the metal center geometry affects Ir-Cl bond length (2.3950(6) Å, Cl-Ir-Si: 131.76(2)°), which is notably shorter than the one found *trans* to silicon atom in [Ir(H)Cl($\kappa^3$-NSiN)(coe)] (2.5229(10) Å, Cl-Ir-Si: 170.51(4)°).[20]

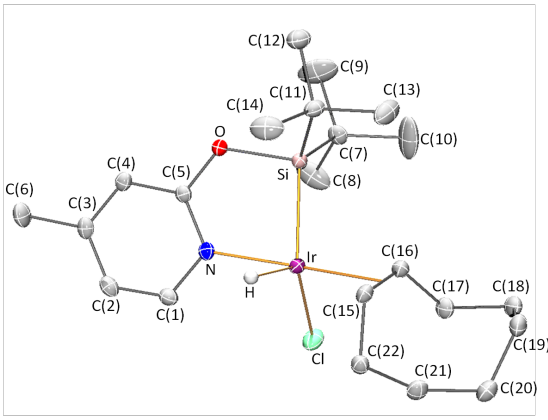


**Figure 1.** Molecular structure of complex **2**: Selection of bond distances (Å ) and angles (°): Ir-Cl, 2.3950(6); Ir-Si, 2.2853(6); Ir-N, 2.0947(18); Ir-Ct 2.0612(15); Ir-H, 1.61; Cl-Ir-Si, 131.76(2); Cl-Ir-N, 88.47(5); Cl-Ir-Ct$^a$, 97.44(4); Cl-Ir-H, 123.8; Si-Ir-N, 81.72(6); Si-Ir-Ct, 98.42(5); Si-Ir-H, 100.0; N-Ir-Ct, 171.74(5); N-Ir-H, 77.8; Ct-Ir-H, 94.1. Ct is the centroid of the olefinic bond of coe ligand.

The reaction of complex **2** with one equivalent of the silver salt $AgCF_3SO_3$ in $CH_2Cl_2$, quantitatively affords the expected transmetalation product [Ir(H)($CF_3SO_3$)($\kappa^2$-NSi$^{tBu}$)(coe)] (**3**), which has been isolated as a yellow solid in 75% yield, and characterized by elemental analysis and NMR spectroscopy (Scheme 2).

$^1$H NMR spectra of complexes **2** and **3** show the signal assigned to the Ir-H proton as a singlet at δ -20.68 and -27.46 ppm, respectively. The coordination of the olefin to the iridium atom is corroborated by two multiplets resonances corresponding to the CH protons of the coe ligand, which appear at δ 4.82 and 3.39 ppm (**2**), and δ 4.93 and 3.58 ppm (**3**). In agreement with the solid structure determined for complex **2** (Figure 1) the two $^t$Bu groups of complexes **2** and **3** are no equivalent in solution. Thus, two singlet resonances for the $^t$Bu protons at δ 1.11 and 1.00 ppm and δ 1.20 and 0.96 ppm where observed in the $^1$H NMR spectra of complexes **2** and **3**, respectively. These findings support that the structure of **3** could be similar to that found for **2** (Figure 1). The remaining resonances of the $^1$H and $^{13}$C{$^1$H} NMR spectra agree with the structure proposed for these complexes. The $^{29}$Si{$^1$H} NMR spectra of **2** and **3** show a singlet resonance at δ 41.9 (**2**) and 45.8 ppm (**3**), which is low field shifted with respect to the resonance observed for **1**. Moreover, the presence of the $CF_3$ in complex **3** has been confirmed by $^{19}$F{$^1$H} NMR spectroscopy, which shows a singlet resonance at δ -78.55 ppm.

**Ir-NSi$^{tBu}$ catalyzed reduction of formamides with hydrosilanes. Optimization of the catalytic conditions.** $^1$H NMR studies of the reaction of *N*-formylpyrrolidine with two equivalents of $HSiMe_2Ph$ at 298 K in presence of catalytic amounts of **2** or **3**

(5.0 mol%) evidenced that both catalysts promote the selective reduction of *N*-formylpyrrolidine to *N*-methylpyrrolidine. In the case of the **2**-catalyzed (5.0 mol%) reactions the immediate formation of $(CH_2)_4NCH_2OSiMe_2Ph$ (**4a**), which was slowly transformed into $(CH_2)_4NMe$ (**5a**), was observed (Scheme 3). However, using **3** (5.0 mol%) as catalyst precursor the reaction of *N*-formylpyrrolidine with two equivalents of $HSiMe_2Ph$ did not evidence the formation of **4a** along the reaction. This could suggest that in presence of **3** the transformation of **4a** into **5a** is faster than in the case of the **2**-catalyzed reactions. In agreement with that the full conversion of *N*-formylpyrrolidine into **5a** using **3** was achieved in 1 h, while using **2** as catalyst precursor 4 h were required. $^1H$ and $^{29}Si\{^1H\}$ NMR spectra of these reactions confirm that the starting $HSiMe_2Ph$ is transformed into the corresponding siloxane $O(SiMe_2Ph)_2$.

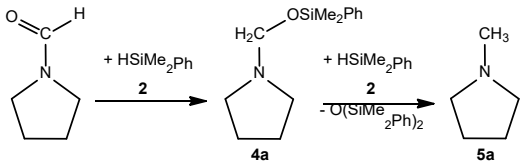


Scheme 3. Catalyzed reduction of *N*-formylpyrrolidine with $HSiMe_2Ph$ in presence of catalytic amounts (5.0 mol%) of complex **2**. Using complex **3** the formation of **4a** could not be observed.

Moreover, the $^1H$ NMR spectra of the above described catalytic reactions evidence the presence of a single resonance at δ 1.50 ppm, which correlates in the $^1H$-$^{13}C$ HSQC with a resonance that appears in the $^{13}C\{^1H\}$ NMR spectra at δ 27.0 ppm, due to cyclooctane resulting from the hydrogenation of the coe ligand, as well as the formation of unidentified iridium-hydride intermediate species, which agrees with the need for a catalyst activation step.

To explore the effect of the catalyst loading we have performed experiments using 0.5 mol% of complexes **2** and **3**. $^1H$ NMR studies of the **2**-catalyzed (0.5 mol%) reaction of *N*-formylpyrrolidine with two equivalents of $HSiMe_2Ph$ at 298 K show that, analogously to the above-described experiments done in presence of 5.0 mol% of **2**, the fast transformation of *N*-formylpyrrolidine into **4a** takes place during the first minutes of the reaction. Afterwards the slow transformation of **4a** into **5a** is observed (Figure 2). Under the same reaction conditions, 298 K, $C_6D_6$ and two equivalents of $HSiMe_2Ph$, complex **3** (0.5 mol%) promote the reduction of *N*-formylpyrrolidine to afford **5a** (Figure 3). In this case, similarly to that observed for the **3**-catalyzed (5.0 mol%) reaction, **5a** was the only reaction product observed along the reaction. Therefore, these findings allow to conclude that using a catalyst loading of 0.5 mol% of complexes **2** and **3** it is possible to achieve a reasonable catalytic activity.

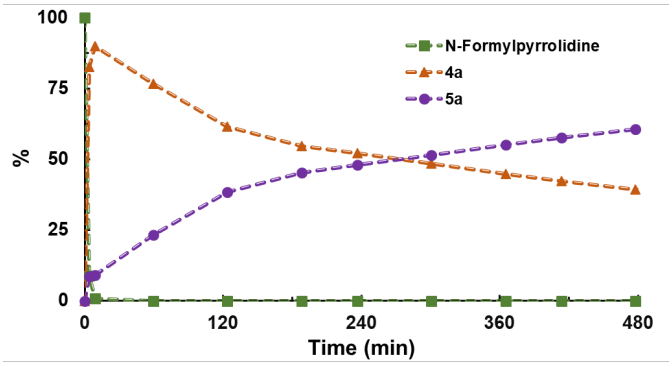


**Figure 2.** Kinetic profile of the **2**-catalyzed (0.5 mol%) reaction of *N*-formylpyrrolidine with two equivalents of $HSiMe_2Ph$ in $C_6D_6$ at 298K. The discontinuous lines only represent a connection between the data points.

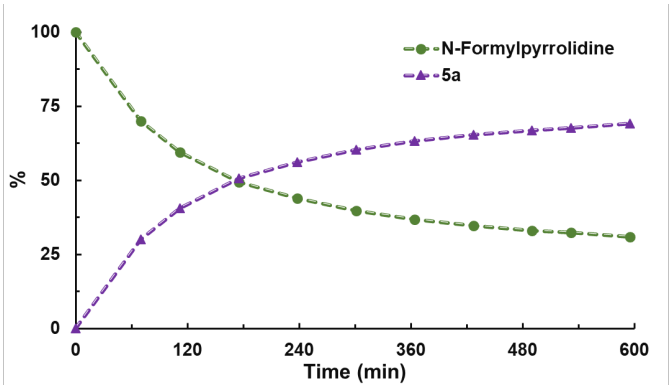


**Figure 3.** Kinetic profile of the **3**-catalyzed (0.5 mol%) reaction of *N*-formylpyrrolidine with two equivalents of $HSiMe_2Ph$ in $C_6D_6$ at 298K. The discontinuous lines only represent a connection between the data points.

**Catalytic reaction of formamides with $HSiMe_2Ph$ in presence of 2 (0.5 mol%).** *O*-silylated hemiaminals have been proposed as highly reactive intermediates in the reduction of amides to amines with silanes,[3j,12c,25] Therefore, the above-described results found for **2** aimed us to explore its potential application as catalyst for the synthesis of *O*-silylated hemiaminals from the reaction of formamides with one equivalent of $HSiMe_2Ph$ (Table 1). $^1H$ NMR studies of the **2**-catalyzed (0.5 mol%) reaction of $C_6D_6$ solutions of *N*-formylpyrrolidine, dimethylformamide, N-methyl-N-phenyl-formamide with one equivalent of $HSiMe_2Ph$ at 298K show the quantitative formation of the corresponding *O*-silylated hemiaminal, $(CH_2)_4NCH_2OSiMe_2Ph$ (**4a**), $Me_2NCH_2OSiMe_2Ph$ (**4b**) $MePhNCH_2OSiMe_2Ph$ (**4c**), which was selectively obtained (>99%) after 0.8 h, 6 h and 24 h, respectively. In the case of *N*,*N*-diphenylformamide the reaction was also found to be selective to the formation of the corresponding *O*-silylated hemiaminal, however, it is much more slower than that carried out using the above mentioned formamides. Indeed, after 24 h after reaction only 50 % of conversion was observed. Under the same reaction conditions, the selective reduction of *N*,*N*-diisopropylformamide could not be achieved. Indeed, after 16 hours of reaction 82% of conversion of the formamide to give a mixture of the corresponding *O*-silylated hemiaminal $Me_2PhSiOCH_2N^iPr_2$ (**4e**)

(80%) and *N,N*-diisopropylmethylamine (**5e**) (20%) was observed. A different behavior was observed when complex **3** was used as catalyst precursor. Thus, the **3**-catalyzed reactions of formamides with one equivalent of $HSiMe_2Ph$ afford mixtures of the starting formamide and the corresponding methylamine. These results agree with the above-described higher activity of **3** in comparison with **2** as hydrosilylation catalysts.

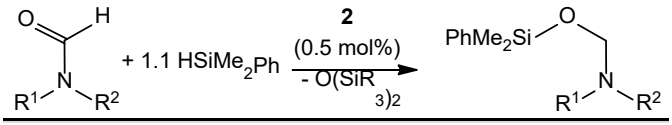


**Table 1.** Results from the reaction of formamides with $HSiMe_2Ph$ in $C_6D_6$ at 298K using **2** (0.5 mol%) as catalyst precursor.

| formamide | Time (h) | Hemiaminal (%)[a] | $TOF_{1/2}$ ($h^{-1}$) |
|---|---|---|---|
| *N*-formylpyrrolidine | 0.8 | >99 | 750 |
| *N,N*-dimethylformamide | 6.0 | >99 | 240 |
| *N*-methyl-*N*-phenylformamide | 24 | 98 | 15 |
| *N,N*-diphenylformamide | 24 | 50 | 4.2 |
| *N,N*-diisopropylformamide | 16.0 | >80[b] | 600 |

[a] % were calculated by $^1H$ NMR integration; [b] 82% of conversion based on the starting formamide to afford a mixture 4:1 of the corresponding *O*-silylated hemiaminal and methylamine, respectively.

It should be mentioned that the reaction temperature influences the selectivity of the **2**-catalyzed (0.5 mol%) reaction of *N*-formylpyrrolidine with one equivalent of $HSiMe_2Ph$. Indeed, heating at 323 K, under the above-described conditions, the formation of **5a** as side reaction product together with **4a** could not be avoided. Thus, the best selectivities to the corresponding *O*-silylated hemiaminal were obtained at 298 K.

In the case of the **2**-catalyzed (0.5 mol%) reactions of $C_6D_6$ solutions of *N*-formylpyrrolidine, *N,N*-dimethylformamide or *N,N*-diisopropylformamide with 2.1 equivalents of $HSiMe_2Ph$ the full conversion of the starting formamide into the corresponding *O*-silylated hemiaminal takes place in few minutes (Figure 2). However, the subsequent reduction of the hemiaminal was found to be very slow. Indeed, after 14 h only an 80%, 15% or 23% of the corresponding methylamine was observed.

**3-catalyzed (0.5 mol%) reduction of amides to the corresponding amine.** The **3**-catalyzed (0.5 mol%) reaction of *N*-formylpyrrolidine with one equivalent of $HSiMe_2Ph$ affords an equimolar mixture of the corresponding methylamine and the starting *N*-formylpyrrolidine. The above described outcomes prompted us to explore the potential of complex **3** as catalyst precursor for the reduction of formamides with $HSiMe_2Ph$. Thus, the reactions of *N*-formylpyrrolidine, *N,N*-dimethylformamide, *N*-methyl-*N*-phenylformamide, *N,N*-diphenylformamide and *N,N*-diisopropylformamide with 2.1 equivalents of $HSiMe_2Ph$ in presence of **3** (0.5 mol%) were comparatively studied by $^1H$ NMR spectroscopy in $C_6D_6$ at 323 K (Table 2).

These studies allow to conclude that using a low loading of **3** (0.5 mol%) it is possible to achieve the selective reduction of *N*-formylpyrrolidine, *N,N*-dimethylformamide, *N*-methyl-*N*-phenylformamide, *N,N*-diphenylformamide and *N,N*-diisopropylformamide to quantitatively afford the corresponding methylamine, which was characterized by comparison of their $^1H$, $^{13}C\{^1H\}$ NMR spectra with those reported in the literature (Table 2).

The performance of the catalytic reactions depends very much on the nature of the formamide. Indeed, few minutes are required to transform *N*-formylpyrrolidine into N-methylpyrrolidine while hours were needed to complete the reduction of the others formamides (Table 2). This behavior could be due to a complex balance of electronic and steric factors. For instance, it draws attention that the reduction of *N,N*-dimethylformamide requires more time than that of *N,N*-diisopropylformamide. This could not be attributable to steric factors since the *N*-formyl group is more hindered in the later than in *N,N*-dimethylformamide.

The higher activity found for *N,N*-diisopropylformamide in comparison with *N,N*-dimethylformamide as well as the poor reactivity observed for *N,N*-diphenylformamide in comparison with *N*-methyl-*N*-phenylformamide (Table 2) shows that the nucleophilic character of the oxygen atom of the formyl group, independently of the steric hinderance around the nitrogen atom, exerts a positive effect on the catalytic activity of the catalytic systems based on **2** and **3**. This suggests that the iridium-$NSi^{tBu}$ promoted reduction of formamides with $HSiMe_2Ph$ could take place via no-classic mechanisms,[26] similar to those proposed for other iridium based catalysts.[12]

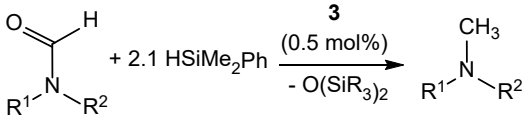


**Table 2.** Results from the reaction of amides with $HSiMe_2Ph$ in $C_6D_6$ at 323K using **3** (0.5 mol%) as catalyst precursor.

| formamide | Time (h) | Amine (%)[a] | $TOF_{1/2}$ ($h^{-1}$) |
|---|---|---|---|
| N-formylpyrrolidine | 0.25 | >99 | 4000 |
| *N,N*-dimethylformamide | 8.5 | >99 | 50 |
| *N*-methyl-*N*-phenylformamide | 15 | 90 | 120 |
| *N,N*-diphenylformamide | 15 | 70 | 15 |
| *N,N*-diisopropylformamide | 2.5 | >99 | 343 |

[a] % were calculated by $^1H$ NMR integration.

$^1H$ NMR studies show that in absence of formamide complexes **2** and **3** react with excess of $HSiMe_2Ph$ (4 equivalents) to afford mixtures of unidentified hydride species, cyclooctane and traces of free cyclooctene. Under the same conditions the

reaction of complex **2** with $HSiMe_2Ph$ is slower than with **3**. These results agree with the outcomes from the catalytic studies and show that the ancillary ligand exerts a relevant role in the catalyst activation step, which in the case of the triflate derivative **3** is faster than for **2**.

It has been observed that using **2** the reduction of formamides to the corresponding *O*-silylated hemiaminal is faster than the subsequent reduction of the *O*-silylated hemiaminals to the corresponding methylamine. Conversely, when **3** was used as catalysts the corresponding *O*-silyl hemiaminal was never observed, which shows that in this case the first reduction is slower than the second one. This differw behaviour could be the reason behind the highly selectivity to *O*-silyl hemiaminas found for **2** (Scheme 4).

Therefore, the overall catalytic process could be understood as a three steps process involving; (i) catalyst activation, (ii) reduction of formamide to *O*-silylated hemiaminal and (iii) reduction of the *O*-silylated hemiaminal to the corresponding methylamine.

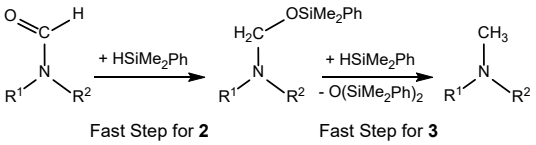


Scheme 4. Representation of the rate control step of the **2**- and **3**-catalyzed reduction of formamides with $HSiMe_2Ph$.

## Experimental

### General Considerations

All experiments and manipulations were carried out under rigorous exclusion of air using Schlenk-type techniques and MBraun glovebox when necessary. Solvents were dried and distilled under argon by standards procedures prior to use or purified by a Solvent Purification System (Innovative Technologies). NMR spectra were obtained on a Bruker ARX-300, Bruker AV-300 MHz or Varian Gemini 2000. Chemical shifts ($\delta$), reported in ppm, were referenced to the residual peaks of deuterated solvents. The amides and the silicon-hydrides were purchased from commercial sources. The amides were dried over A4 molecular-sieves.

**4-Methylpyridine-2-yloxydi*tert*butylsilane (1).** A solution of $HSi^tBu_2Cl$ (1.50 mL, 7.42 mmol) in THF (10 mL) was slowly added to a THF solution (10 mL) of 2-hydroxy-4-methylpyridine (0.80 g, 7.33 mmol) and imidazole (0.58 g, 8.52 mmol) at RT. After the addition the resulting mixture was stirred during 5h. Then the solvent was removed in vacuo. The product was extracted with pentane (3 x 5 mL) and dried under reduced pressure to afford a pale-yellow oil. Yield: 1.69 g (92 %). High Resolution Mass Spectrometry ($ESI^+$): calc. *m/z* = 252.1778; found *m/z* = 252.1782 ($M^+$). $^1H$ NMR (300 MHz, $CD_2Cl_2$, 298 K): δ 7.95 (m, 1H, $C_6$-H), 6.72 (m, 1H, $C_5$-H), 6.57 (m, 1H, $C_3$-H), 4.50 (s, 1H, Si-H), 2.28 (s, 3H, py-$CH_3$), 1.06 (s, 18H, Si-$^t$Bu). $^{13}C\{^1H\}$ NMR (75 MHz, $CD_2Cl_2$, 298 K): δ 163.3 (s, $C_2$), 151.0 (s, $C_4$), 147.3 (s, $C_6$), 119.0 (s, $C_5$), 113.2 (s, $C_3$), 27.5 (s, *C*$H_3$-$^t$Bu), 21.0 (s, py-*C*$H_3$), 20.2 (s, Si-C). $^{29}Si\{^1H\}$ NMR (HMBC $^{29}Si$-$^1H$, 298 K): δ 12.0.

**Synthesis of [Ir(Cl)(H)($\kappa^2$-NSi$^{tBu}$)(coe)] (2).** A solution of compound **1** (0.500 g, 1.988 mmol) in $CH_2Cl_2$ (5 mL) was slowly added to a suspension of $[IrCl(coe)_2]_2$ (0.890 g, 0.993 mmol) in $CH_2Cl_2$ (10 mL) at 273 K. The mixture was then stirred at room temperature for 16h. The solvent was removed in vacuo and the residue was precipitated with pentane (3 x 5 mL) at 195 K. The washing solutions were combined and dried in vacuo to afford a bright-yellow solid. Yield: 0.860 g (73.4%). Anal. Calcd. for $C_{22}H_{39}ClIrNOSi$: C, 44.84; H 6.67; N 2.38. Found: C 44.85; H 6.70; N 2.62. $^1H$ NMR (300 MHz, $CD_2Cl_2$, 298 K): δ 8.43 (m, 1H, $C_6$-H), 6.79 (s, 1H), 6.75 (m, 1H, $C_3$-H), 4.82 (m, 1H, CH-coe), 3.39 (m, 1H, CH-coe), 2.47 (m, 2H , $CH_2$-coe), 2.32 (m, 3H, py-$CH_3$), 2.19 – 1.97 (m, 2H, $CH_2$-coe), 1.89 – 1.20 (m, 8H, $CH_2$-coe), 1.11 (s, 9H , Si-$^t$Bu), 1.00 (s, 9H, Si-$^t$Bu), -20.68 (s, 1H, Ir-H). $^{13}C\{^1H\}$ NMR (75 MHz, $CD_2Cl_2$, 298 K): δ 154.3 (s, $C_4$), 147.6 (s, $C_6$), 117.5 (s, $C_5$), 111.0 (s, $C_3$) 71.2 (s, CH-coe), 62.0 (s, CH-coe), 31.2 (s, $CH_2$-coe), 30.5 (s, $CH_2$-coe), 29.4 (s, *C*$H_3$-$^t$Bu), 28.4 (s, *C*$H_3$-$^t$Bu), 27.1 (s, $CH_2$-coe), 26.3 (s, $CH_2$-coe), 26.1 (s, $CH_2$-coe), 24.8 (s, Si-C), 24.1 (s, Si-C), 21.0 (s, py-*C*$H_3$). $^{29}Si\{^1H\}$ NMR (HMBC $^{29}Si$-$^1H$, 298 K): δ 41.9.

**Synthesis of [Ir($CF_3SO_3$)(H)($\kappa^2$-NSi$^{tBu}$)(coe)] (3)**. $CH_2Cl_2$ (10 mL) was added to a light-protected Schlenk containing **2** (0.300 g, 0.510 mmol) and silver triflate (0.150 g, 0.583 mmol). The resulting mixture was stirred for 5h at room temperature. The solution was filtered through Celite and dried in vacuo, the residue was then washed with pentane (3 x 5 mL) to afford a yellow solid. Yield: 270 mg (75%). Anal. Calcd. for $C_{23}H_{39}F_3IrNO_4SSi$: C, 39.3; H, 5.59; N, 1.99; S, 4.56. Found: C, 39.01; H, 5.76; N, 1.88; S, 4.49. $^1H$ NMR (300 MHz, $CD_2Cl_2$, 298 K): δ 8.17 (m, 1H, $C_6$-H), 6.87(s, 1H, $C_3$-H), 6.82 (m, 1H, $C_3$-H), 4.93 (m, 1H, CH-coe), 3.58 (m, 1H, CH-coe), 2.37 (s, 3H, py-$CH_3$), 2.30 – 1.25 (m, 12H, $CH_2$-coe), 1.20 (s, 9H, Si-$^t$Bu), 0.96 (s, 9H, Si-$^t$Bu), -27.46 (s, 1H, Ir-H). $^{13}C\{^1H\}$ NMR (75 MHz, $CD_2Cl_2$, 298 K): δ 156.4 (s, $C_4$), 147.9 (s, $C_6$), 118.5 (s, $C_5$), 112.1 (s, $C_3$), 76.3(s, CH-coe), 68.5 (s, CH-coe), 31.6 (s, $CH_2$-coe), 30.4 (s, $CH_2$-coe), 29.8 (s, *C*$H_3$-$^t$Bu + $CH_2$-coe), 28.4 (s, *C*$H_3$-$^t$Bu), 26.8 (s, $CH_2$-coe), 26.5 (s, $CH_2$-coe), 26.2 (s, $CH_2$-coe), 24.8 (s, Si-C), 21.88 (s, py-$CH_3$). $^{29}Si\{^1H\}$ NMR (HMBC $^{29}Si$-$^1H$, 298 K): δ 45.8. $^{19}F\{^1H\}$ NMR (282 MHz, $CD_2Cl_2$): δ -78.55.

**Catalytic reaction of *N*-Formylpyrrolidine with $HSiMe_2Ph$ in presence of catalytic amounts of species 2, and 3 (5 mol %).** In a glovebox the catalyst precursor **2** was added to an NMR tube (5.0 mg, 8.48 µmol) and dissolved in $C_6D_6$ (0.5 mL). *N*-formylpyrrolidine (16.2 µL, 16.9 mmol) and $HSiMe_2Ph$ (54.5 µL, 35.5 mmol) were added to this solution and the resulting mixture was studied by NMR spectroscopy. The same process was followed with complex **3** (5.0 mg**,** 7.11 µmol).

**Reaction of different amides with $HSiMe_2Ph$ in presence of complexes 2 or 3 (0.5 mol %).**

The desired amount of amide (0.254 mmol) and the corresponding equivalents of $HSiMePh_2$ (1 eq., 0.254 mmol; 2

eq., 0.534 mmol) were added to an NMR tube. To this a $C_6D_6$ solution (0.5 mL) of complex **2** (0.75 mg, 1.27 µmol) was added and the resulting mixture was studied by NMR spectroscopy. The same process was followed with complex **3** (0.75 mg**,** 1.07 µmol).

**Selected NMR data of the products.**

$(CH_2)_4NCH_2OSiMe_2Ph$ (**4a**): $^1$H NMR (300 MHz, $C_6D_6$, 298 K): δ 7.61. 7.24 (m, 5H, Si-Ph), 4.52 (s, 2H, $CH_2$-O), 2.75 (m, 4H, N-$CH_2$), 1.60 (m, 4H, N-$CH_2$), 0.35 (s, 6H, $SiMe_2$). $^{13}C\{^1H\}$ NMR (75 MHz, $C_6D_6$, 298 K): δ 77.5 (s, N-$CH_2O$), 48.8 (s, N-$CH_2$), 24.9 (s, $CH_2$) -1.3 (s, SiMe). $^{29}Si\{^1H\}$ NMR (HMBC $^{29}Si$-$^1H$, 298 K): δ 4.7.

$Me_2NCH_2OSiMe_2Ph$ (**4b**): $^1$H NMR (300 MHz, $C_6D_6$, 298 K): δ 7.59. 7.24 (m, 5H, Si-Ph), 4.31 (s, $CH_2$, 2H), 2.29 (s, N-$CH_3$, 3H), 0.33 (s, Si-$CH_3$, 6H). $^{13}C\{^1H\}$ NMR (75 MHz, $C_6D_6$, 298 K): δ 82.6 (s, $CH_2$), 41.2 (s, N-$CH_3$), -1.36 (s, Si-$CH_3$). $^{29}Si\{^1H\}$ NMR (HMBC $^{29}Si$-$^1H$, 298 K): δ 4.5.

$PhMeNCH_2OSiMe_2Ph$ (**4c**): $^1$H NMR (300 MHz, $C_6D_6$, 298 K): δ 7.52 (m, Ph), 7.19 (m, Ph), 6.83 (m, Ph), 4.78 (s, 2H, $CH_2$), 2.62 (s, 3H, N-$CH_3$), 0.26 (s, 6H, $SiMe_2$). $^{13}C\{^1H\}$ NMR (75 MHz, $C_6D_6$, 298 K): δ 148.8, 138.2, 133.9, 129.9, 129.3, 128.2, 118.8, 114.7 (s, pH), 77.8 (s, $CH_2$), 37.6 (s, N-$CH_3$), -1.3 (s, Si-$CH_3$).$^{29}Si\{^1H\}$ NMR (HMBC $^{29}Si$-$^1H$, 298 K): δ 5.3.

$Ph_2NCH_2OSiMe_2Ph$ (**4d**): $^1$H NMR (300 MHz, $C_6D_6$, 298 K): δ 5.16 (s, 2H, $CH_2$), 0.17 (s, 6H, Si-$CH_3$). $^{13}C\{^1H\}$ NMR (75 MHz, $C_6D_6$, 298 K): δ 77.1 (s, $CH_2$), -1.4 (s, Si-$CH_3$). $^{29}Si\{^1H\}$ NMR (HMBC $^{29}Si$-$^1H$, 298 K): δ 6.2.

$^iPr_2NCH_2OSiMe_2Ph$ (**4e**): $^1$H NMR (300 MHz, $C_6D_6$, 298 K): δ 4.61 (s, 2H, $CH_2$), 3.11 (sp, *J* = 6.6 Hz, 2H, $^i$Pr), 1.11 (d, *J* = 6.6 Hz, 12 H, $^i$Pr), 0.34 (s, 6H, Si-$CH_3$). $^{13}C\{^1H\}$ NMR (75 MHz, $C_6D_6$, 298 K): δ 73.3 (s, $CH_2$), 48.8 (s, N-CH), 22.9 (s, $^i$Pr), -1.2 (s, Si-$CH_3$). $^{29}Si\{^1H\}$ NMR (HMBC $^{29}Si$-$^1H$, 298 K): δ 1.7.

$(CH_2)_4NCH_3$ (**5a**): $^1$H NMR (300 MHz, $C_6D_6$, 298 K): δ 2.34 (m, 4H, N-$CH_2$), 2.25 (s, 3H, $CH_3$), 1.63 (m, 4H, $CH_2$). $^{13}C\{^1H\}$ NMR (75 MHz, $C_6D_6$, 298 K): δ 56.5 (s, N-$CH_2$), 42.3 (s, N-$CH_3$), 24.6 (s, $CH_2$).

$N(CH_3)_3$ (**5b**): $^1$H NMR (300 MHz, $C_6D_6$, 298 K): δ 2.07 (s, 9H, $CH_3$). $^{13}C\{^1H\}$ NMR (75 MHz, $C_6D_6$, 298 K): δ 47.7 (s, N-$CH_3$).

$PhN(CH_3)_2$ (**5c**): $^1$H NMR (300 MHz, $C_6D_6$, 298 K): δ 7.27 – 7.19 (m, 2H, Ph), 6.77 (t, *J* = 7.3 Hz, 1H, Ph), 6.64 (d, 2H, Ph), 2.55 (s, 6H, N-$CH_3$). $^{13}C\{^1H\}$ NMR (75 MHz, $C_6D_6$, 298 K): δ 129.4, 117.1, 113.1 (s, Ph), 40.3 (s, N-$CH_3$).

$Ph_2NCH_3$ (**5d**) $^1$H NMR (300 MHz, $C_6D_6$, 298 K): δ 2.93 (s, N-$CH_3$). $^{13}C\{^1H\}$ NMR (75 MHz, $C_6D_6$, 298 K): δ 40.1 (s, N-$CH_3$).

$^iPr_2NCH_3$ (**5e**): $^1$H NMR (300 MHz, $C_6D_6$, 298 K): δ 2.84 (sp, *J* = 6.5 Hz, 2H, N-CH), 2.09 (s, 3H, N-$CH_3$), 0.97 (d, J = 6.5 Hz, 12H, $CH_3$). $^{13}C\{^1H\}$ NMR (75 MHz, $C_6D_6$, 298 K): δ 50.7 (s, N-CH), 30.9 (s, N-$CH_3$), 20.2 (s, $CH_3$).

**Crystal Structure Determination of Complex 2.**

Single crystal X-ray diffraction data were collected at 100(2) K with graphite-monochromated Mo Kα radiation (λ=0.71072 Å) using narrow frame rotation (Δω=0.3°) on a Bruker Smart APEX diffractometer. Measured intensities were integrated and corrected for absorption effects with SAINT+[27] and SABABS[28] programs, included in APEX3 package. The structure was solved with direct methods with SHELXS-2013[29] and refined by full-matrix least-squares refinement on $F^2$ with SHELXL-2017[30] program, included in WingX package.[31] Several refinement strategies have been tested for hydride ligand refinement. Its free refinement from observed position leads to unrealistic geometrical parameters (Si-Ir-H: 64.1 degree angle). Moreover, no evidence of agostic interactions has been observed in NMR spectra. Therefore, hydride ligand position has been calculated from consideration of the molecular geometry and a potential energy minimization calculation with HYDEX program.[32] Calculated position has been fixed and the isotropic atomic displacement parameter has been constrained to be 1.5 times the Ueq of the metal atom. CCDC 1857508 contains the supplementary crystallographic data for this paper. These data can be obtained free of charge from The Cambridge Crystallographic Data Centre via www.ccdc.cam.ac.uk/structures.

**Crystal data compound 2.** $C_{22}H_{39}ClIrNOSi$, *M* = 589.28; yellow prism 0.080 x 0.090 x 0.240 mm$^3$; triclinic $P\bar{1}$, *a* = 8.8806(4), *b* = 10.5584(4), *c* = 12.7712(5) Å, *α*=94.4790(10), *β*=91.3980(10), *γ* =94.6700(10)°, *V* = 1189.30(8) Å$^3$; *Z* = 2; $D_c$ = 1.646 g/cm$^3$; *μ* = 5.788 mm$^{-1}$; 17208/5722 reflections measured/unique ($R_{int}$ = 0.0172), number of data/restraint /parameters 5722/0/258, $R_1(F^2)$ = 0.0172 (5534 reflections, $I > 2\sigma(I)$) and w$R(F^2)$ = 0.0404 (all data), final *GoF* = 1.101, largest difference peak: 1.156 e.Å$^{-3}$.

## Conclusions

The reaction of 4-methylpiridin-2-iloxy-di*terc*butyl silane (**1**) with of $[IrCl(coe)_2]_2$ (coe = *cis*-cyclooctene) affords the Ir(III) complex [Ir(H)(Cl)($\kappa^2$-NSi$^{tBu}$)(coe)] (**2**), which has been fully characterized inluding X-ray diffracction studies. The reaction of **2** with one equivalent of $Ag(CF_3SO_3)$ gives [Ir(H)($CF_3SO_3$)($\kappa^2$-NSi$^{tBu}$)(coe)] (**3**).

Complexes **2** and **3** catalyze the reduction of formamides with hydrosilanes. Interestingly, at 298 K using **2** (0.5 mol%) as catalyst it has been possible to selectively obtain the corresponding *O*-silylated hemiacetal derivative by reaction of a number of formamides with one equivalent of $HSiMe_2Ph$. On the other hand, complex **3** (0.5 mol%) has shown to be an effective catalyst precursor for the selective reduction of formamides to the corresponding methylamine by reaction with two equivalents of $HSiMe_2Ph$. The performance of the catalytic system based on **2** and **3** strongly depends of the formamide. Thus, both catalysts were highly active for the reduction of *N*-formylpyrrolidine to the the corresponding *O*-silylated hemiacetal (**2**) or to *N*-methylpyrrolidine (**3**) using the stoichiometric ammount of $HSiMe_2Ph$. However, a decrease of activity was observed for the catalytic reactions with *N,N*-dimethylformamide and *N,N*-diisopropylformamide. Moreover, formamides with aromatic substituents, *N*-methyl-*N*-phenylformamide and *N,N*-diphenylformamide, were found to be less reactive than the above-mentioned formamides. This could be due to the delocalization of the nitrogen lone pair on the aromatic rings.

In summary, the ancillary ligand plays a key role on the selectivity of the Ir-NSi$^{tBu}$-catalyzed reduction of formamides with hydrosilanes. Thus, complex **2** with a chloride ligand allows the selective preparation of *O*-silylated hemiaminals, while species **3**, with a triflate ancillary ligand, promotes the selective

reduction of formamides to the corresponding methylamine. In addition, these catalytic systems operate under low catalyst loading and without the need for extra additives.

## Conflicts of interest

"There are no conflicts to declare"

## Acknowledgements

Financial support from MINECO/FEDER project CTQ2015-67366-P and DGA/FSE group E07 is gratefully acknowledged. Dr. P. García-Orduña acknowledges CSIC, European Social Fund and Ministerio de Economía y Competitividad of Spain for a PTA contract. Authors would like to acknowledge the use of Servicio General de Apoyo a la Investigación-SAI, Universidad de Zaragoza.

## References

1 (a) L. Huang, M. Arndt, K. Gooßen, H. Heydt, L. J. Gooßen, *Chem. Rev.* 2015, **115**, 2596-2697; (b) Q. Yang, Q. Wang, Z. Yu, *Chem. Soc. Rev.* 2015, **44**, 2305-2329.

2 G. W. Gribble, *Chem. Soc. Rev.* 1998, **27**, 395-404.

3 For recent reviews see: (a) S. Das, S. Zhou, D. Addis, S. Enthaler, K.Junge, M. Beller, *Top. Catal.* 2010, **53**, 979-984; (b) P. A. Dub, T. Ikariya, *ACS Catal.* 2012, **2**, 1718-1741; (c) S. Werkmeister, K. Junge, M. Beller, *Org. Process Res. Dev.* 2014, **18**, 289-302; (d) E. Balaraman, D. Milstein, *Top. Organomet. Chem.* 2014, **48**, 19-43; (e) J. M. John, R. Loorthuraja, E. Antoniuk, S. H. Bergens, *Catal. Sci. Technol.* 2015, **5**, 1181-1186; (f) J. R. Cabrero-Antonino, E. Alberico, K. Junge, H. Junge, M. Beller, *Chem. Sci.* 2016, **7**, 3432-3442; (g) J. R. Cabrero-Antonino, E. Alberico, H. J. Drexler, W. Baumann, K. Junge, H. Junge, M. Beller, *ACS Catal.* 2016, **6**, 47-54; (h) M. L. Yuan, J. H. Xie, S. F. Zhu, Q. L. Zhou, *ACS Catal.* 2016, **6**, 3665-3669; (i) M. L. Yuan, J. H. Xie, Q. L. Zhou, *ChemCatChem* 2016, **8**, 3036-3049; (j) B. Li, J.-B. Sortais, C. Darcel, *RSC Adv.* 2016, **6**, 57603-57625; (k) A. Chardon, E. Morisset, J. Rouden, J. Blanchet, *Synthesis* 2018, **50**, 984-987.

4 (a) R. Calas. E. Frainnet, A. Bazouin. *C. R. Acad. Sci.* 1962, **254**, 2357-2359; (b) for a review see: R. Calas, *J. Organomet. Chem.* 1980, **200**, 11-36.

5 R. Kuwano, M. Takahashi, Y. Ito, *Tetrahedron Lett.*, 1998, **39**, 1017-1020.

6 K. Selvakumar, K. Rangaredly, J. F. Harrod, *Can. J. Chem.*, 2004, **82**, 1244-1248.

7 (a) A. Volkov, F. Tinnis, T. Slagbrand, I. Pershagen, H. Adolfsson, *Chem. Commun.*, 2014, **50**, 14508-14511; (b) S. Krackl, C. I. Someya, S. Enthaler, *Chem. Eur. J.*, 2012, **18**, 15267-15271; (c) A. C. Fernandes, C. C. Romao, *J. Mol. Catal. A: Chem.*, 2007, **272**, 60-63.

8 (a) X. Frogneux, O. Jacquet, T. Cantat, *Catal. Sci. Tecnol.*, 2014, **4**, 1529-1533; (b) A. Volkov, E. Buitrago, H. Adolfsson, *Eur. J. Org. Chem.*, 2013, 2066-2070; (c) B. Blom, G. Tan, S. Enthaler, S. Innoue, J. D. Epping, M. Dries, *J. Am. Chem. Soc.,* 2013, **135**, 18108-18120; (d) S. Das, B. Wendt, K. Möller, K. Junge, M. Beller, *Angew. Chem. Int. Ed.*, 2012, **51**, 1662-1666; (e) Y. Sunada, H. Kawakami, T. Imaoka, Y. Motoyama, H. Nagashima, *Angew. Chem. Int. Ed.* 2009, **48**, 9511-9514; (f) S. Zhou, K. Junge, D. Addis, S. Das, M. Beller, *Angew. Chem. Int. Ed.* 2009, **48**, 9507-9510.

9 (a) Y. Li, T. Jan, K. Junge, M. Beller, *Angew. Chem. Int. Ed.*, 2014, **53**, 10476-10480; (b) Y.Li, I. Sorribes, T. Yan, K. Junge, M. Beller, *Angew. Chem. Int. Ed.*, 2013, **52**, 12156-12160; (c) K. Beydoun, T. vom Stein, J. Klankermayer, W. Leitner, *Angew. Chem. Int. Ed.*, 2013, **52**, 9554-9557; (d) Y. Li, X. Fang, K. Junge, M. Beller, *Angew. Chem. Int. Ed.*, 2013, **52**, 9568-9571; (e) B. Li, J.-B. Sortais, C. Darcel, *Chem. Commun.,* 2013, **49**, 3691-3693; (f) J. T. Reeves, Z. Tan, M. A. Marsini, Z. S. Han, Y. Xu, D. C. Reeves, H. Lee, B. Z. Lu, C. H. Senanayake, *Adv. Synth. Catal.*, 2013, **355**, 47-52; (g) S. Hanada, T. Ishida, Y. Motoyama, H. Nagashima, *J. Org. Chem.* 2007, **72**, 7551-7559; (h) H. Sasakuma, Y. Motoyama, H. Nagashima, *Chem. Commun.*, 2007, 4916-4918; (i) Y. Motoyama, C. Itonaga, T. Ishida, M. Takasaki, H. Nagashima, *Org. Synth.*, 2005, **82**, 188-195; (j) Y. Motoyama, K. Mitsui, T. Ishida, H. Nagashima, *J. Am. Chem. Soc.*, 2005, **127**, 13150-131151; (k) K. Matsubara, T. Iura, T. Maki, H. Nagashima, *J. Org. Chem.*, 2001, **67**, 4985-4988.

10 T. Dombray, C. Helleu, C. Darcel, J.-B. Sortais, *Adv. Synth. Catal.*, 2013, **355**, 3358-3362.

11 (a) C. Bornschein, A. J. J. Lennox, S. Werkmeister; K. Junge, M. Beller, *Eur. J. Org. Chem.*, 2015, 1915-1919; (b) S. Das, Y. Li, C. Bornschein, S. Pisiwicz, K. Kiersch, D. Michalik, F. Gallou, K. Junge, M. Beller, *Angew. Chem. Int. Ed.*, 2015, **54**, 12389-12393; (c) M. Stoelzel, C. Präsang, B. Blom, M Driess, *Aust. J. Chem.*, 2013, **66**, 1163-1170.

12 (a) Y. Corre, X. Trivelli, F. capet, J.-P. Djukic, F. Agbossou-Niedercorn, C. Michon, *ChemCatChem*, 2017, **9**, 2009-2017; (b) A. Tahara, Y. Miyamoto, R. Aoto, K. Shigeta, Y. Une, Y. Sunada, Y. Motoyama, H. Nagashima, *Organometallics*, 2015, **34**, 4895-4907; (c) S. Park, M. Brookhart, *J. Am. Chem. Soc.*, 2012, **134**, 640-653; (d) C. Cheng, M. Brookhart, *J. Am. Chem. Soc.*, 2012, **134**, 11304-11307; (e) Y. Motoyama, M. Aoki, N. Takaoka, R. Aoto, H. Nagashima, *Chem. Commun.*, 2009, 1574-1576.

13 (a) S. Pisiewicz, K. Junge, M. Beller, Eur. J. Inorg. Chem., 2014, 2345-2349; (b) S. Hanada, E. Tsutsumi, Y. Motoyama, H. Nagashima, *J. Am. Chem. Soc.*, 2009, **131**, 15032-15040; (c) S. Hanada, Y. Motoyama, H. Nagashima, *Tetrahedron Lett.*, 2006, **47**, 6173-6177.

14 S. Das, B. Join, K. Junge, M. Beller, *Chem. Commun.*, 2012, **48**, 2683-2685.

15 (a) O. O. Kovalenko, A. Volkov, H. Adolfsson, *Org. Lett.*, 2015, **17**, 446-449; (b) O. Jacquet, X. Frogneux, C. Das Neves Gomes, T. Cantat, *Chem. Sci.*, 2013, **4**, 2127-2131, (c) S. Das, D. Addis, K. Junge, M. Beller, *Chem. Eur. J.*, 2011, **17**, 12186-12192; (d) S. Das, D. Addis, S. Zhou, K. Junge, M. Beller, *J. Am. Chem. Soc.*, 2010, **132**, 1770-1771.

16 F. J. Fernández-Alvarez, R. Lalrempuia, L. A. Oro, *Coord. Chem. Rev.*, 2017, **350**, 49-60.

17 (a) A. Julián, J. Guzmán, E. A: Jaseer, F. J. Fernández-Alvarez, R. Royo, V. Polo, P. García-Orduña, F. J. Lahoz, L. A. Oro, *Chem. Eur. J.,* 2017, **23**, 11898-11907; (b) A. Julián, E. A. Jaseer, K. Garcés, F. J. Fernández-Alvarez, P. García-Orduña, F. J. Lahoz, L. A. Oro, *Catal. Sci.Technol.*, 2016, **6**, 4410-4417; (c) R. Lalrempuia, M. Iglesias, V. Polo, P. J. Sanz Miguel, F. J. Fernández-Alvarez, J. J. Pérez-Torrente, L. A. Oro, *Angew. Chem. Int. Ed.*, 2012, **51**, 12824–12827.

18 A. Julián, V. Polo, E. A. Jaseer, F. J. Fernández-Alvarez, L. A. Oro, *ChemCatChem,* 2015, **7**,3895 –3902.

19 A. Julián, V. Polo, F. J. Fernández-Alvarez, L. A. Oro, *Catal. Sci. Technol.*, 2017, **7**, 1372–1378.

20 A. Julián, K. Garcés, R. Lalrempuia, E. A. Jaseer, P. García-Orduña, F. J. Fernández-Alvarez, F. J. Lahoz, L. A. Oro, *ChemCatChem*, 2018, **10**, 1027–1034.

21 K. Garcés, R. Lalrempuia, V. Polo, F. J. Fernández-Alvarez, P. García-Orduña, F. J. Lahoz, J. J. Pérez-Torrente, L. A. Oro, *Chem. Eur.J.* 2016, **22**, 14717-14729.

22 L. Ehrlich, R. Gericke, E. Brendler, J. Wagler, *Inorganics* 2018, ,**6**, 119.
23 D. Cremer, J. A. Pople, *J. Am. Chem. Soc*., **1975**, *97*, 1354-1358.
24 C. R. Groom, I. J. Bruno, M. P. Lightfot, S. C. Ward, *Acta Crystallogr*. **2016**, *B72*, 171-179.
25 (a) L.-G. Xie, D. J. Dixon, *Nature Commun.*, 2018, **9**, article number 2841; (b) P. E. Gonzalez, H. K. Sharma, S. Chakrabarty, A. Metta-Magaña, K. H. Pannell, *E. J. Org. Chem.*, **2017**, 5610-5616; (c) H. K. Sharma, P. E. Gonzalez, A. L. Craig, S. Chakrabarty, A. Metta-Magaña, K. H. Pannell, *Chem. Eur. J.,* **2016**, *22*, 7363-7366; (d) J. L. Martinez, H. K. Sharma, R. Arias-Ugarte, K. H. Pannell, *Organometallics*, **2014**, *33*, 2964-2967; (e) H. K. Sharma, R. Arias-Ugarte, D. Tomlinson, R. Gappa, A. J. Metta-Magaña, H. Ito, K. H. Pannell, *Organometallics*, **2013**, *32*, 3788-3794; (f) R. Arias-Ugarte, H. K. Sharma, A. L. C. Morris, K. H. Pannell, *J. Am. Chem. Soc.*, **2012**, *134*, 848-851; (g) S. Krackl, C. I: Someya, S. Enthaler, *Chem. Eur. J.*, **2012**, *18*, 15267-15271.
26 M. Iglesias, F. J. Fernández- Alvarez, L. A. Oro, *Coord. Chem. Rev.* **2019**, doi: 10.1016/j.ccr.2019.02.003.
27 SAINT+, version 6.01: Area-Detector Integration Software, Bruker AXS, Madison 2001.
28 SADABS 2016/02. L. Krause, R. Herbst-Irmer, G. M. Sheldrick, D. Stalke, *J. Appl. Crystallogr*., **2015**, *48*, 3-10.
29 (a) G. M. Sheldrick, *Acta Crystallogr*. *A*, **1990**, *46*, 467-473; (b) G. M. Sheldrick, *Acta Crystallogr*. *A*, **2008**, *64*, 112-122.
30 G. M. Sheldrick, *Acta Crystallogr*. *C*, **2015**,*71*, 3-8.
31 L. J. Farrugia, *J. Appl. Crystallogr*., **2012**,*45*, 849-854.
32 A. G. Orpen, *J. Chem. Soc. Dalton Trans*., **1980**, 2509-2516.